Physicochem. Probl. Miner. Process., 62(1), 2025, 217036

http://www.journalssystem.com/ppmp

Physicochemical Problems of Mineral Processing

ISSN 1643-1049

Separation of fine lepidolite from quartz by reverse flotation using sodium metaphosphate as depressant

Liuyi Ren [1,2,3], Pengfei Song [1,2], Shenyi Li [1,2], Shenxu Bao [1,2,3], Yimin Zhang [1,2,3,4,5], Xinyu Zhang [1,2], Yali Zhang [6]

[1] Key Laboratory of Green Utilization of Critical Non-metallic Mineral Resources, Ministry of Education, Wuhan University of Technology

[2] School of Resources and Environmental Engineering, Wuhan University of Technology, Wuhan 430070, China

[3] Hubei Key Laboratory of Mineral Resources Processing and Environment, Wuhan 430070, China

[4] State Environmental Protection Key Laboratory of Mineral Metallurgical Resources Utilization and Pollution Control, Wuhan University of Science and Technology, Wuhan 430081, China

[5] Hubei Collaborative Innovation Center for High Efficient Utilization of Vanadium Resources, Wuhan University of Science and Technology, Wuhan 430081, China

[6] School of Geography and Tourism, Xinjiang Normal University, Urumqi 830054 Xinjiang, China

Corresponding author: rly1015@163.com, rly1015@whut.edu.cn (Liuyi Ren)

Abstract: Amid growing global demand for lithium resources, the efficient recovery of lepidolite has gained significant attention. However, fine-grained lepidolite particles often remain underutilized in conventional beneficiation processes due to their poor floatability and high surface energy. Therefore, it is essential to develop effective methods for separating fine lepidolite from associated gangue minerals. In this study, we systematically investigated the flotation behavior of fine lepidolite (–20 μm) and quartz (–40 μm) in the presence of depressants. The separation mechanism was elucidated through micro-flotation tests, zeta potential analysis, adsorption capacity measurements, wettability studies, and X-ray photoelectron spectroscopy (XPS). The results demonstrate that sodium metaphosphate (SM) acts as an effective depressant for lepidolite in a tetradecyltrimethylammonium chloride (TTAC) system. Under optimized conditions (pH = 7, [TTAC] = 30 mg/L, [SM] = 100 mg/L), a lepidolite concentrate with a Li_2O grade of 2.93% and a recovery of 68.40% was achieved. Mechanism studies revealed that SM competes with TTAC for adsorption sites on lepidolite surfaces, while enhancing TTAC adsorption on quartz. Furthermore, SM exhibits a limited effect on lepidolite, thereby increasing the separation efficiency between quartz and lepidolite. These findings provide theoretical insights into the efficient separation of fine lepidolite from quartz, offering a potential strategy for improving lithium resource utilization.

Keywords: lepidolite, quartz, fine particle flotation, separation, depressant

1. Introduction

Lithium, renowned as the "energy metal" of the 21st century, has emerged as a key enabler of renewable energy technologies owing to its exceptional electrochemical properties. It finds extensive applications in rechargeable lithium-ion batteries, glass and ceramics, lubricants, pharmaceuticals, and other industrial sectors (Sunet al., 2020; Lv et al., 2018). Driven by the rapid expansion of the new energy industry, global lithium demand has risen sharply from 265 kilotons in 2015 to a projected 498 kilotons by 2025 (Choubey et al., 2017; Liu et al., 2019). In response, diverse strategies are being developed to improve both lithium production and product quality. Currently, lithium is primarily extracted from brine, spodumene, and lepidolite (Kesler et al., 2012; Swain, 2017; Yao et al., 2019). Among these, lepidolite is characterized by its relatively low lithium content and fine-grained mineral structure, which complicate its processing. As a result, the selective enrichment of lithium from

DOI: 10.37190/ppmp/217036

lepidolite has attracted increasing research attention (Wang et al., 2020; Dang et al., 2020; Gu et al., 2020).

Lepidolite, as a lithium-bearing aluminosilicate mineral, is commonly separated from gangue minerals via flotation, which remains the most effective beneficiation technique for this purpose (Wills and Finch, 2016; Liu et al., 2019; Xu et al., 2016). The performance of the flotation process is highly dependent on the selection and combination of reagents, including collectors, depressants, activators, and regulators (Gao et al., 2016; Feng et al., 2018; Liu et al., 2019). Given that lepidolite is often intergrown with quartz and feldspar, the development of collectors that exhibit both high selectivity and strong collecting power has become a major research priority (Vieceli et al., 2016; Vieceli et al., 2017). Dodecylamine (DDA), a typical cationic collector, is widely employed in the flotation of mica-group minerals such as lepidolite (Dey et al., 2020; Zhu et al., 2018; Zhu et al., 2020; Jara et al., 2020). For example, Pung et al. (Pugh et al., 1996) studied the influence of pH on mica flotation using DDA as the collector and correlated the flotation response with the stability of thin aqueous foam films and surface force measurements. However, although DDA shows strong collecting ability, it suffers from poor selectivity and ill-defined separation efficiency in mixed mineral systems (Xu et al., 2014). Moreover, effective separation of lepidolite from quartz or feldspar generally requires highly acidic conditions (pH=2–3), which lead to high sulfuric acid consumption, severe equipment corrosion, complicated wastewater treatment, and potential environmental impacts. As a result, lepidolite flotation under such strongly acidic environments is often considered economically unviable (Wei et al., 2021).

Recently, the application of mixed collectors—including anionic/cationic, anionic/non-ionic, and cationic/non-ionic combinations—has gained increasing interest for enhancing flotation performance (Marion et al., 2015; Xu et al., 2020). Xu et al. reported that a mixed system of sodium oleate (NaOL) and dodecylamine hydrochloride (DDA) yielded superior mica flotation results compared to the use of either collector alone (Xu et al., 2016). Similarly, Buatovic achieved muscovite mica recoveries between 70% and 96.5% using a blend of oleic/linoleic acid and tallow amine acetate, which outperformed oleic acid by itself (Bulatovic, 2007). In another study, a combination of the cationic collector cetyltrimethylammonium chloride (CTAC) and the non-ionic collector octanol (OCT) demonstrated a synergistic effect, leading to higher muscovite recovery over a broad pH range compared to individual reagents (Yang et al., 2018). Wang et al. further showed that NaOL/DDA mixed collector enabled effective separation of muscovite from quartz at pH 10 (Wang et al., 2014). Complementing these findings, our research group has systematically investigated mica recovery improvement through grinding optimization and crystal chemistry analysis (Ren et al., 2023; Fan et al., 2023; Hao et al., 2023; Ren et al., 2024).

While current lepidolite flotation research explores various surfactant combinations, few studies have systematically addressed the reverse flotation separation of fine lepidolite from quartz and feldspar. In this work, TTAC was employed as a quartz collector. We systematically evaluated the depressant effects of various depressants on the flotation behavior of fine-grained talc and quartz under different pH conditions. An in-depth discussion was also provided on the flotation responses of lepidolite and quartz in a near-neutral pH environment. The underlying separation mechanisms were further elucidated using zeta potential measurements, adsorption capacity tests, wettability analysis, and X-ray photoelectron spectroscopy (XPS).

2. Materials and methods

2.1. Sample and reagents

In this study, high-purity lepidolite ore from Pakistan and quartz samples from Yunnan Province, China, were utilized. Chemical composition analysis (Table 1) and X-ray diffraction (XRD, Fig. 1) confirmed that both minerals possessed purities exceeding 93%, thereby satisfying the experimental requirements. The lepidolite ore was ground in a stirred mill for 55 minutes, yielding particles with a D_{90} of 19.67 μm. Similarly, quartz was processed using a ball mill to obtain fine particles with a D_{90} of 39.95 μm. The particle size distributions of both materials are presented in Fig. 2.

All chemical reagents used in this study were of analytical grade. TTAC and SM were supplied by Shanghai Macklin Biochemical Co., Ltd. (China). The pH values of the solutions were adjusted using dilute NaOH or HCl, and all experiments were conducted with ultrapure water (electrical resistivity >18.2 MΩ·cm).

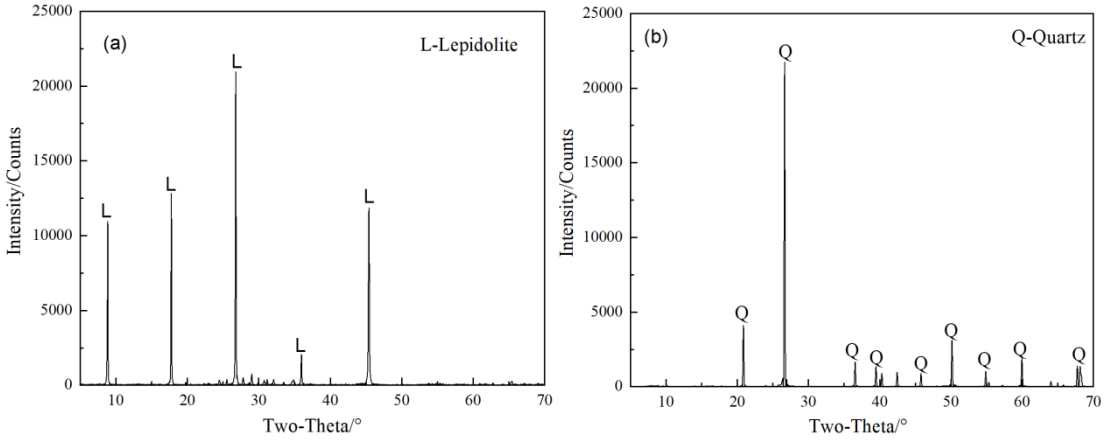

Fig. 1. X-ray diffraction pattern of lepidolite (a) and quartz (b)

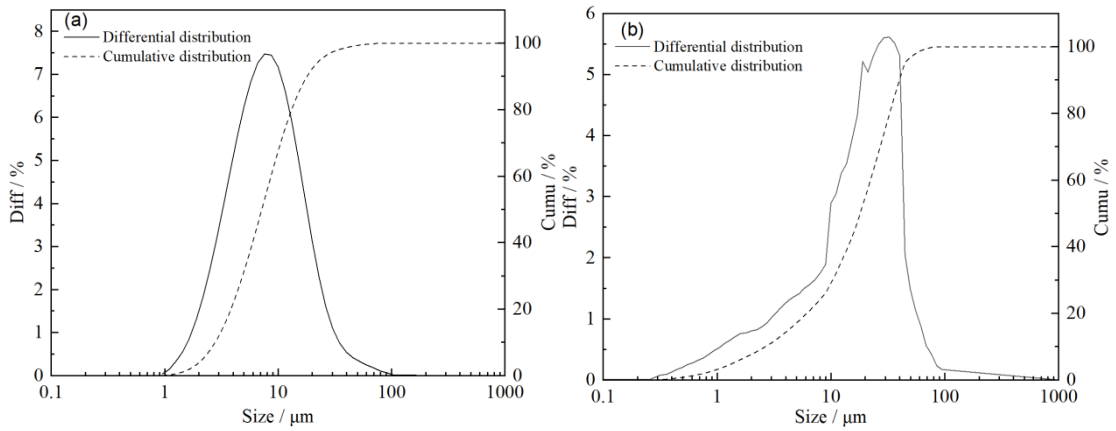

Fig. 2. Particle size distribution curve of lepidolite (a)and quartz (b)

Table 1. Chemical composition of lepidolite and quartz / %

Mineral	Li_2O	SiO_2	Al_2O_3	K_2O	Na_2O	Fe_2O_3
lepidolie	4.72	47.51	26.88	9.75	0.361	0.025
quartz	/	97.96	1.53	0.143	0.074	0.030

2.2. Microflotation tests

Micro-flotation tests were performed using an XFG II flotation machine (Jilin Prospecting Machinery Plant, China) operated at a fixed impeller speed of 1800 rpm. The flotation machine generated bubbles ranging from 0.5 mm to 3 mm in size, with the dominant bubble population between 1 mm and 2 mm. This size range matches well with the particle size of the minerals, indicating that the bubbles are capable of capturing the majority of the mineral particles (Zhuo et al., 2020). The reagent conditioning sequence and corresponding durations are schematically illustrated in Fig. 3. In each test, a mineral suspension was prepared by agitating the pulp for 2 min. The pH was subsequently adjusted with diluted HCl or NaOH, followed by 3 min of conditioning. Depressants and the collector TTAC were then introduced sequentially, each followed by a 3-min conditioning period. Froth products were collected by manual scraping over 6 min. Both concentrates and tailings were dried, weighed, and used to calculate mineral recovery.

For flotation of mixed minerals, a 1:1 blend of lepidolite and quartz (total mass 2.0 g) was thoroughly homogenized prior to testing. The flotation procedure and reagent addition scheme remained consistent with the single-mineral tests. After flotation, all products were collected, dried, and weighed. The Li_2O

content in the concentrates and tailings was determined by chemical analysis, and recovery was calculated based on both mass distribution (yield) and Li_2O grade.

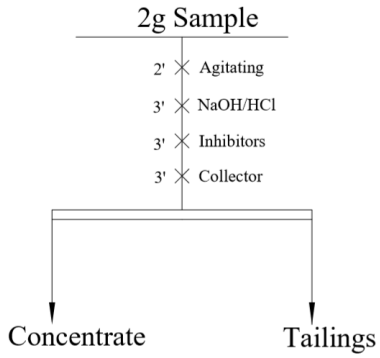

Fig. 3. Flowsheet of micro-flotation experiment

2.3. Zeta potential measurements

The zeta potentials of lepidolite and quartz were measured by Nano-ZS90 instrument (Malvern Panalytical, UK). Measurements were carried out in ultrapure water, TTAC solution (60 mg/L), and depressant solution (100 mg/L) across a pH range of 2–12. Mineral particles finer than 10 μm were used for all tests, which were conducted at 25 °C. Prior to each measurement, the suspension was magnetically stirred for 15 min and subsequently allowed to settle for 10 min. The supernatant was then collected for zeta potential analysis. All experiments were performed in triplicate, and the reported data represent the average values.

2.4. Adsorption capacity measurements

The concentration of TTAC was determined by ultraviolet-visible (UV–Vis) spectroscopy using a UQQ 2111002 spectrophotometer. The method is based on the colorimetric reaction between eosin Y and TTAC, which produces a concentration-dependent chromogenic complex. A series of standard TTAC solutions with concentrations of 2, 4, 6, 8, 10, and 12 mg/L were prepared as follows. Firstly, appropriate volumes of TTAC stock solution were mixed with 5 mL of HCl–NaAc buffer (pH 4.30) and 10 mL of eosin Y solution. The mixture was then diluted to a final volume of 25 mL using ultrapure water. After 40 min of color development, the absorbance of the resulting TTAC–eosin complex was measured at its maximum absorption wavelength of 550 nm. For the test samples, the supernatant obtained after flotation was collected, transferred to centrifuge tubes, and centrifuged using a high-speed centrifuge. The absorbance was then measured thereafter. As shown in Fig. 4, the absorbance exhibited a linear relationship with TTAC concentration, which was further validated by linear regression analysis.

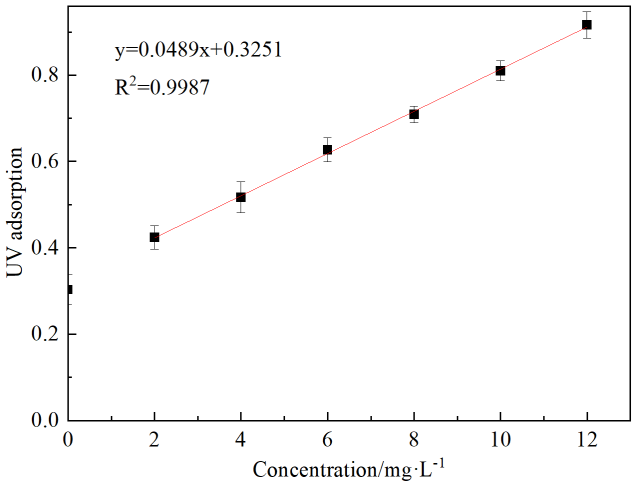

Fig. 4. UV adsorption standard curve for TTAC

2.5. Contact angle measurements

After treatment with flotation reagents, the lepidolite and quartz powders were dried at low temperature and compacted into pellets using a hydraulic press. The hydrophobicity of the mineral surfaces was evaluated by measuring static contact angles with a JC2000D goniometer via the sessile drop method. Ultrapure water droplets were deposited vertically onto the surface, and contact angles were recorded to evaluate the effects of individual reagents and their combinations on surface wettability. All measurements were repeated three times for each condition, and the average values are reported.

2.6. X-ray photoelectron spectroscopy

XPS was utilized to investigate the surface chemical composition and oxidation states of the mineral samples, offering detailed information about their reactivity and adsorption behavior. In this study, test samples were prepared according to three groups of quartz micro-flotation experimental steps, filtered, rinsed and dried at low temperature. XPS measurements were conducted, and spectra were interpreted using Avantage software. All spectra were calibrated using the C1s peak at 284.8 eV.

XPS was utilized to investigate the surface chemical composition and oxidation states of the mineral samples, offering detailed information about their reactivity and adsorption behavior. Three representative flotation-treated samples were filtered and dried before analysis. XPS measurements were conducted, and spectra were interpreted using Avantage software. All spectra were calibrated using the C1s peak at 284.8 eV.

3. Results and discussion

3.1. Microflotation tests results

Flotation experiments were conducted at different slurry pH values using 60 mg/L TTAC and 100 mg/L depressant. The results are presented in Fig. 5. As shown in Fig. 5(a), lepidolite recovery remained stable at 85% across the tested pH range when using TTAC alone or in combination with WG/OA. In the presence of both TTAC and SM, however, lepidolite recovery decreased with increasing pH, reaching a minimum at pH 8. Subsequently, the recovery increased as the pH was further raised. Fig. 5(b) shows that quartz achieved about 90% in the pH range of 4.0–12.0 using TTAC as the collector. The depressants (WG, SM, or OA) showed no inhibitory effect on quartz within this pH range, although a weak depressive effect was observed at pH 2.0.

The depressive effects of different depressant concentrations were evaluated at pH 7.0, as summarized in Fig. 6. Fig. 6(a) demonstrates that lepidolite recovery declined markedly with increasing SM concentration until it stabilized. When the SM concentration exceeded 100 mg/L, lepidolite recovery remained constant. In contrast, Fig. 6(b) shows that quartz recovery was largely unaffected by the variation in SM concentration. Under the condition of 100 mg/L SM, lepidolite recovery was 52.16%, whereas quartz recovery reached 96.63%.

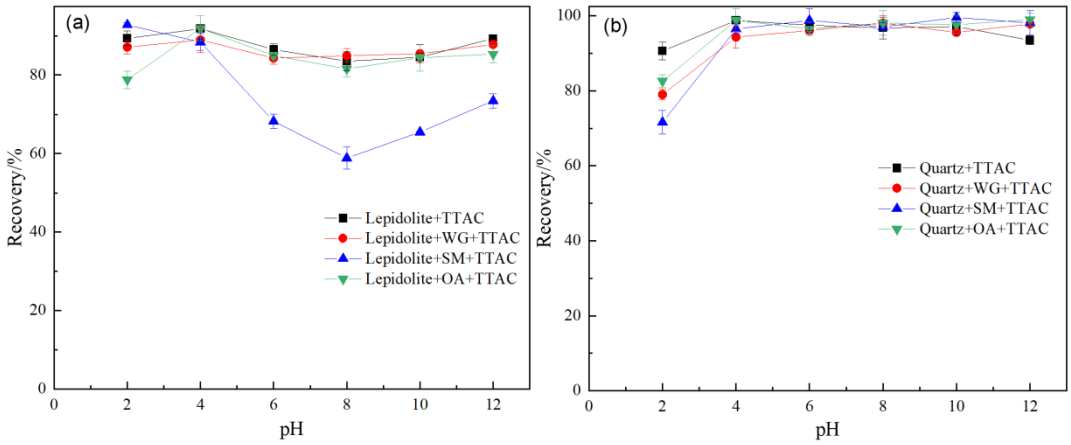

Fig. 5. Flotation recovery of lepidolite (a) and quartz (b) as a function of pH in the absence and presence of depressants (concentration of TTAC: 60 mg/L, depressant: 100mg/L)

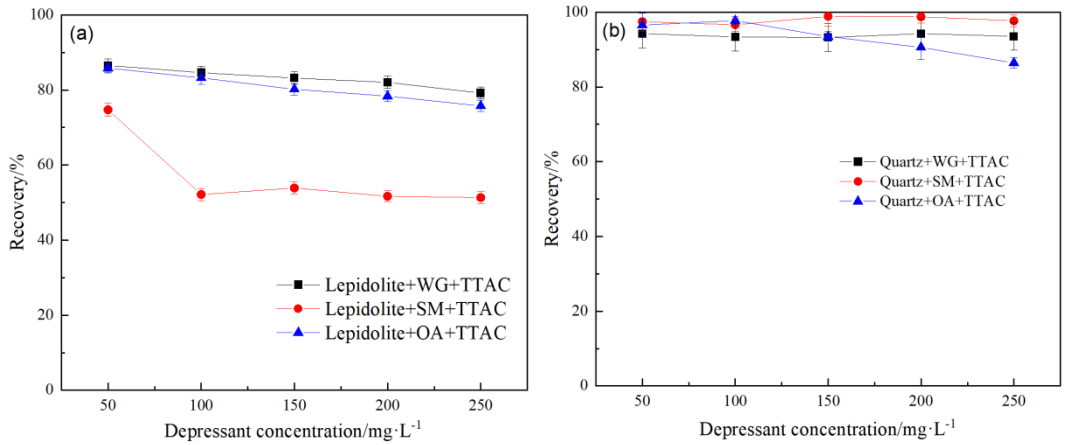

Fig. 6. Effect of depressants on lepidolite(a) and quartz(b) recovery. (pH= 8, concentration of TTAC: 60 mg/L)

Table 2. Flotation results of artificial mixed minerals

TTAC/ mg·L^{-1}	SM/ mg·L^{-1}	Products	Yield/%	Li_2O grade/%	Li_2O recovery/%
30	0	Concentrate	71.34	2.13	64.56
		Tailing	28.66	2.92	35.44
		Feed	100.00	2.36	100.00
	100	Concentrate	44.91	1.66	31.60
		Tailing	55.09	2.93	68.40
		Feed	100.00	2.36	100.00

To evaluate the separation performance of lepidolite from quartz under single-collector versus collector-depressant systems, artificial mixture tests were conducted using a 1:1 mass ratio of lepidolite to quartz, with 30 mg/L TTAC as the collector and 100 mg/L SM as the depressant. Results (Table 2) indicate: Without depressant, lepidolite and quartz show poor separation efficiency. With SM addition, Li_2O grade increased from 2.36% to 2.93%, while Li_2O recovery reached 68.40%. This confirms SM's selective depressant of lepidolite in reverse flotation, enabling effective quartz-lepidolite separation.

3.2. Zeta potential measurement results

The zeta potentials of lepidolite and quartz under different reagent conditions are shown in Fig. 7(a) and 7(b). The isoelectric point (IEP) of lepidolite was observed between pH 2 and 4, whereas quartz exhibited strongly negative surface charges (ζ < -30 mV) across the entire pH range of 2–12. The addition of TTAC caused a pronounced positive shift in the zeta potentials of both minerals, confirming the electrostatic adsorption of the cationic collector. In contrast, the addition of SM together with TTAC significantly reduced their zeta potentials at pH < 8, indicating effective adsorption of SM onto both mineral surfaces.

3.3. Effect of pH and SM on the adsorption capacity of TTAC

The adsorption capacity of TTAC on lepidolite and quartz was measured across a range of pH values, using a fixed TTAC concentration of 60 mg/L and SM concentration of 100 mg/L. As shown in Fig. 8, the adsorption capacity of TTAC on lepidolite first decreased and then increased with rising pH. At pH < 6, it decreased sharply; between pH 6 and 8, it remained stable; and above pH 8, it increased gradually. This trend aligns well with the flotation recovery behavior of lepidolite shown in Fig. 5(a). In contrast, the adsorption capacity of TTAC on quartz exhibited an opposite trend with pH. Notably, the

adsorption capacity of TTAC on lepidolite was significantly higher than that on quartz. This difference can be explained by two main reasons. First, quartz exhibits higher natural floatability than lepidolite when using TTAC as the collector, resulting in greater flotation recovery even at low collector concentrations. Second, lepidolite has a finer particle size (D_{90} = 19.67 μm) compared to quartz (D_{90} = 39.95 μm), which likely provides a larger specific surface area and thus enhances its adsorption capacity for TTAC, as noted earlier in Section 2.1.

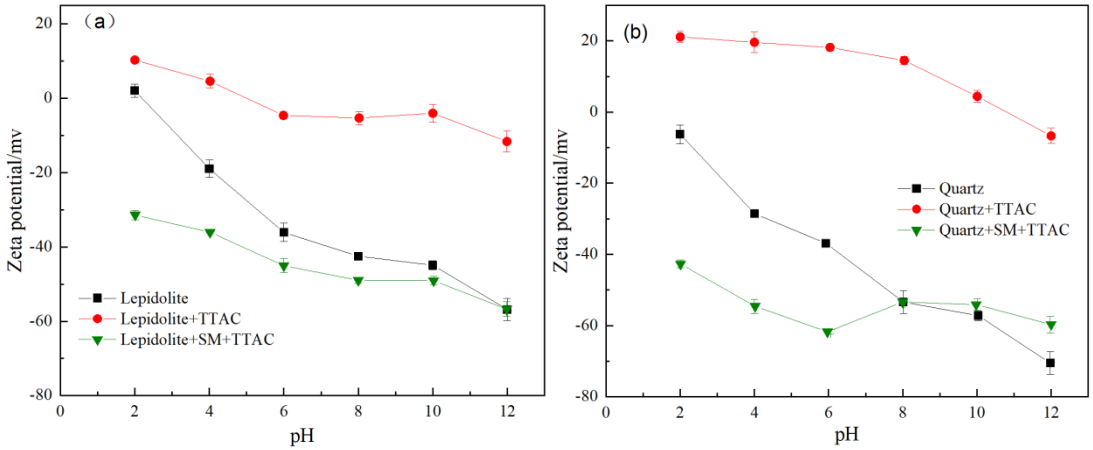

Fig. 7. Effects of depressant on Zeta potential of lepidolite (a) and quartz (b) particle (concentration of TTAC: 60 mg/L，SM: 100mg/L)

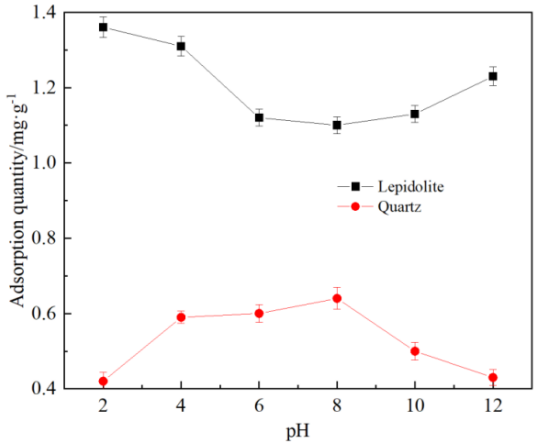

Fig. 8. Relationship of pH value and the adsorption capacity of TTAC on minerals (concentration of TTAC: 60 mg/L, SM: 100 mg/L)

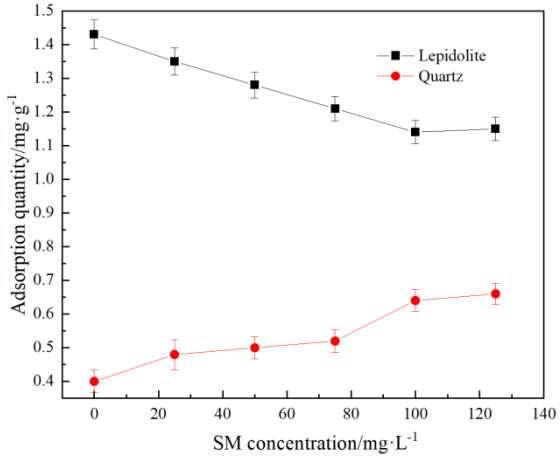

Fig. 9. Adsorption capacities of TTAC at different concentrations of SM (concentration of TTAC: 60 mg/L)

To further elucidate the mechanism by which SM influences TTAC adsorption, the adsorption capacities of TTAC on lepidolite and quartz were measured at different SM concentrations and a fixed pH of 7.0. As shown in Fig. 9, the adsorption capacity of TTAC on lepidolite progressively declined with increasing SM concentration up to 100 mg/L, indicating competitive adsorption between SM and TTAC on the lepidolite surface. This competition suppressed TTAC adsorption, thereby contributing to the reduced flotation recovery of lepidolite. At SM concentrations exceeding 100 mg/L, TTAC adsorption on lepidolite reached a plateau. In contrast, TTAC adsorption on quartz exhibited a modest increase with rising SM concentration, suggesting that SM facilitates the adsorption of TTAC on quartz. Similarly, when SM concentration exceeded 100 mg/L, TTAC adsorption on quartz also stabilized. These results confirm that 100 mg/L is the optimal SM dosage, which is consistent with the earlier flotation findings.

3.4. Wettability analysis of lepidolite and quartz

The surface wettability of lepidolite and quartz was evaluated by contact angle measurements under different reagent conditions. As illustrated in Fig. 10, the contact angles of both minerals were compared in the presence of TTAC alone and in combination with SM. In the case of lepidolite (Fig. 10a), the addition of SM resulted in a sharp decrease in the contact angle, especially in the pH range of 4–10, indicating enhanced surface hydrophilicity. In contrast, quartz (Fig. 10b) showed no significant change in contact angle across the tested pH range upon SM addition, confirming that SM has minimal influence on quartz wettability. These results further support the selective depressive effect of SM on lepidolite, which is consistent with its role in facilitating effective separation from quartz during flotation.

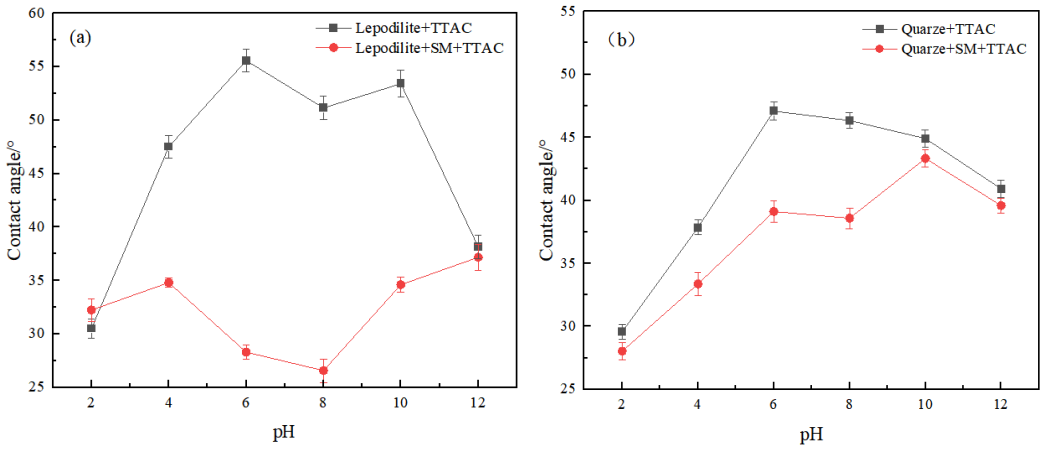

Fig. 10. Contact angles of lepidolite (a) and quartz (b) as a function of pH in the presence of TTAC or SM and TTAC (concentration of TTAC: 60 mg/L，depressant: 100mg/L)

The contact angle of lepidolite decreased across the pH range of 4–8, reaching its minimum at pH 8, and subsequently increased gradually with further rise in pH, while remaining essentially unchanged at pH 2 and 10. This trend indicates that the depressive effect of SM on lepidolite is most pronounced at pH 8. Moreover, quartz wettability was scarcely influenced by SM at this pH. These observations are consistent with previous flotation and adsorption results, confirming that pH 6–8 represents the optimal range for effective lepidolite-quartz separation.

3.5. XPS analysis

The XPS results for quartz are summarized in Table 3 and Fig. 11. Although nitrogen is detected on the quartz surface after TTAC treatment, the N content shows no significant difference from that of the reagent-free surface. The full XPS spectrum further revealed no distinct N peak before or after TTAC adsorption, indicating minimal adsorption of TTAC on quartz. In contrast, when SM and TTAC were applied together, clear nitrogen peaks emerged in the XPS spectrum with substantially increased N content, confirming that SM enhances the adsorption of TTAC on the quartz surface.

Table 3. XPS spectra on the molar fraction of each element in quartz before and after reagent solution treatment.

element	molar/%				
	C	N	O	P	Si
Quartz	10.59	0.69	57.82	0.78	30.11
Quartz +TTAC	11.86	0.73	57.14	0.68	29.59
Quartz +SM+TTAC	22.66	1.35	49.84	1.54	24.62

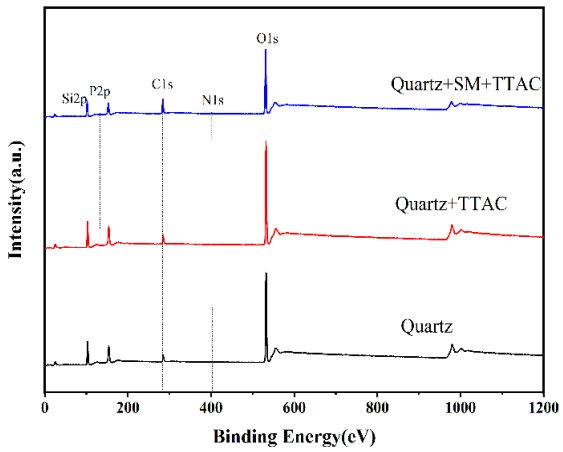

Fig. 11. XPS spectra on quartz surface before and after reagents treatment

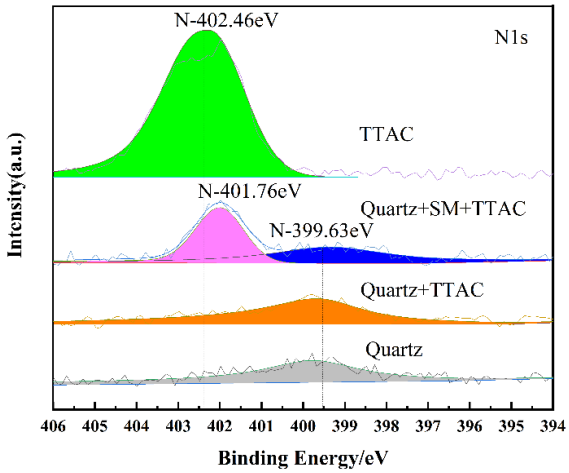

Fig. 12. N1s XPS spectra on quartz surface before and after reagents treatment

As shown in Fig. 12, no new peaks appeared and the binding energy of N1s remained unchanged after TTAC treatment, indicating no significant adsorption of TTAC on the quartz surface. In contrast, following the co-adsorption of SM and TTAC, a new N1s peak emerged at 401.76eV in the quartz spectrum. Comparison with the reference spectrum of pure TTAC, which exhibits an N1s peak at 402.46 eV, reveals a chemical shift of 0.7eV. This shift suggests the formation of a chemisorption bond between TTAC and the quartz surface in the presence of SM. These XPS results are consistent with the flotation experiments, confirming that SM enhances TTAC adsorption on quartz, thereby improving its flotation recovery.

4. Conclusions

(1) Reverse flotation using TTAC as the collector and SM as the depressant successfully separated fine lepidolite from quartz. Optimal performance was achieved at pH 7.0 with 30 mg/L TTAC and 100 mg/L SM, yielding tailings with a Li_2O grade of 2.93% and a recovery of 68.40%.

(2) Mechanistically, SM adsorbs on both minerals but functions selectively: it competes with TTAC on lepidolite surfaces, reducing its adsorption, while promoting TTAC adsorption on quartz. This opposing effect enhances the selectivity of the separation process.
(3) Further evidence was observed at pH 8, where the contact angle of lepidolite reached a minimum—indicating markedly increased wettability—while that of quartz remained stable. Consistent with this, SM was found to significantly enhance TTAC adsorption on quartz. Together with a distinct chemical shift in the XPS N 1s spectra, these results strongly suggest that chemisorption occurs between TTAC and quartz in the presence of SM.

Acknowledgments

The financial support provided by the National Natural Science Foundation of China (52474300, 52274270, U2003129) and Guangxi Regional Innovation Capacity Improvement Program (Collaboration Action Plan) (XT2504240003) is acknowledged.

References

BULATOVIC, S. M., 2007. *Handbook of Flotation Reagents: Chemistry, Theory and Practice*; Elsevier: Amsterdam.

CHOUBEY, P. K., CHUNG, K.-S., KIM, M.-S., LEE, J.-C., SRIVASTAVA, R. R., 2017. *Advance review on the exploitation of the prominent energy-storage element Lithium. Part II: From sea water and spent lithium ion batteries (LIBs)*. Miner. Eng. 110, 104–121.

DANG, H., LI, N., CHANG, Z., WANG, B., ZHAN, Y., WU, X., LIU, W., ALI, S., LI, H., GUO, J., LI, W., ZHOU, H., SUN, C., 2020. *Lithium leaching via calcium chloride roasting from simulated pyrometallurgical slag of spent lithium ion battery*. Sep. Purif. Technol. 233, 116025.

DEY, S., SAHU, L., CHAURASIA, B., NAYAK, B., 2020. *Prospects of utilization of waste dumped low-grade limestone for iron making: A case study.* Int. J. Min. Sci. Technol. 30, 367–372.

FAN, C., REN, L., ZHANG, Y., BAO, S., 2023. *Grinding effect of sodium silicate on muscovite and its mechanism analysis*. Miner. Eng. 199, 108106.

FENG, B., PENG, J., ZHANG, W., NING, X., GUO, Y., ZHANG, W., 2018. *Use of locust bean gum in flotation separation of chalcopyrite and talc.* Miner. Eng. 122, 79–83.

GAO, Z. Y., HU, Y., SUN, W., DRELICH, J. W., 2016. *Surface-charge anisotropy of scheelite crystals.* Langmuir 32, 6282–6288.

GU, H., GUO, T., WEN, H., LUO, C., CUI, Y., DU, S., WANG, N., 2020. *Leaching efficiency of sulfuric acid on selective lithium leachability from bauxitic claystone.* Miner. Eng. 145, 106076.

HAO, J., LIU, J., YU, Y., GAO, H., QIN, X., BAI, X., 2023. *Depressants for separation of chalcopyrite and molybdenite: Review and prospects*. Miner. Eng. 201, 108209.

JARA, A. D., WOLDETINSAE, G., BETEMARIAM, A., KIM, J. Y., 2020. *Mineralogical and petrographic analysis on the flake graphite ore from Saba Boru area in Ethiopia*. Int. J. Min. Sci. Technol. 30, 715–721.

KESLER, S. E., GRUBER, P. W., MEDINA, P. A., KEOLEIAN, G. A., EVERSON, M. P., WALLINGTON, T. J., 2012. *Global lithium resources: Relative importance of pegmatite, brine and other deposits.* Ore Geol. Rev. 48, 55–69.

LIU, C., LIN, J., CAO, H., ZHANG, Y., SUN, Z., 2019. *Recycling of spent lithium-ion batteries in view of lithium recovery: A critical review*. J. Clean. Prod. 228, 801–813.

LIU, C., ZHU, G., SONG, S., LI, H., 2019. *Flotation separation of smithsonite from quartz using calcium lignosulphonate as a depressant and sodium oleate as a collector.* Miner. Eng. 131, 385–391.

LIU, C., ZHANG, W., SONG, S., LI, H., 2019. *A novel method to improve carboxymethyl cellulose performance in the flotation of talc*. Miner. Eng. 131, 23–27.

LV, W., WANG, Z., CAO, H., SUN, Y., ZHANG, Y., SUN, Z., 2018. A *critical review and analysis on the recycling of spent lithium-ion batteries. ACS Sustain.* Chem. Eng. 6, 1504–1521.

MARION, C., JORDENS, A., MCCARTHY, S., GRAMMATIKOPOULOS, T., WATERS, K. E., 2015. *An investigation into the flotation of muscovite with an amine collector and calcium lignin sulfonate depressant*. Sep. Purif. Technol. 149, 216–227.

PUGH, R. J., RUTLAND, M. W., MANEV, E., CLAESSON, P. M., 1996. *Dodecylamine collector – pH effect on mica flotation and correlation with thin aqueous foam film and surface force measurements*. Int. J. Miner. Process. 46, 245–262.

REN, L., JIAO, Z., ZHANG, Y., BAO, S., 2023. *Adsorption difference of octadecylamine on (002) and (131) crystal planes of fine muscovite and its guidance on fine muscovite flotation*. Minerals 13, 519.

REN, L., MA, T., BAO, S., ZHANG, Y., JIAO, Z., ZHANG, X., 2024. *Enhanced flotation performance and adsorption mechanism on (002) crystal plane of fine muscovite powder*. Adv. Powder Technol. 35, 104317.

SUN, S., YU, X., LI, M., DUO, J., GUO, Y., DENG, T., 2020. *Green recovery of lithium from geothermal water based on a novel lithium iron phosphate electrochemical technique*. J. Clean. Prod. 247, 119178.

SWAIN, B., 2017. *Recovery and recycling of lithium: A review*. Sep. Purif. Technol. 172, 388–403.

VIECELI, N., DURÃO, F. O., GUIMARÃES, C., NOGUEIRA, C. A., PEREIRA, M. F. C., MARGARIDO, F., 2016. *Grade-recovery modelling and optimization of the froth flotation process of a lepidolite ore*. Int. J. Miner. Process. 157, 184–194.

VIECELI, N., NOGUEIRA, C. A., PEREIRA, M. F. C., DIAS, A. P. S., DURÃO, F. O., GUIMARÃES, C., MARGARIDO, F., 2017. *Effects of mechanical activation on lithium extraction from a lepidolite ore concentrate*. Miner. Eng. 102, 1–14.

WANG, T., LI, C., XIE, X., et al., 2020. *Anode materials for aqueous zinc ion batteries: Mechanisms, properties, and perspectives.* ACS Nano 14, 16321–16347.

WANG, L., SUN, W., HU, Y., XU, L., 2014. *Adsorption mechanism of mixed anionic/cationic collectors in Muscovite – Quartz flotation system*. Miner. Eng. 64, 44–50.

WEI, Q., FENG, L., DONG, L., JIAO, F., QIN, W., 2021. *Selective co-adsorption mechanism of a new mixed collector on the flotation separation of lepidolite from quartz*. Colloids Surf. A 612, 125973.

WILLS, B. A., FINCH, J., 2016. *Wills' Mineral Processing Technology*, 8th ed.; Butterworth-Heinemann: Oxford.

XU, L., HU, Y., TIAN, J., WU, H., YANG, Y., ZENG, X., WANG, Z., WANG, J., 2016. *Selective flotation separation of spodumene from feldspar using new mixed anionic/cationic collectors.* Miner. Eng. 89, 84–92.

XU, L., HU, Y., TIAN, J., et al., 2016. *Synergistic effect of mixed cationic/anionic collectors on flotation and adsorption of muscovite.* Colloids Surf. A 492, 181–189.

XU, Y., LIU, Y., GAO, S., JIANG, Z., SU, D., LIU, G.-S., 2014. *Monolayer adsorption of dodecylamine surfactants at the mica/water interface.* Chem. Eng. Sci. 114, 58–69.

XU, Y., XU, L., WU, H., WANG, Z., SHU, K., FANG, S., ZHANG, Z., 2020. *Flotation and co–adsorption of mixed collectors octanohydroxamic acid/sodium oleate on bastnaesite*. J. Alloys Compd. 819, 152948.

YANG, Q. H., JIANG, H., JI, W. Y., XIE, J. H., GAO, Y., 2018. *Mechanism of flotation of muscovite using mixed quaternary ammonium salt/octanol collectors.* Chin. J. Nonferrous Met. 28, 1900–1907.

YAO, M., ZHU, J., MENG, W., LI, C., LI, C., WANG, L., JIANG, Z., HE, Z., LI, Y., MENG, W., ZHOU, H., DAI, L., 2019. *Enhanced lithium storage performance of nanostructured $NaTi_2(PO_4)_3$ decorated by nitrogen-doped carbon.* Electrochim. Acta 294, 226–232.

ZHU, G., WANG, Y., WANG, X., YU, F., MILLER, J. D., 2018. *States of coadsorption for oleate and dodecylamine at selected spodumene surfaces.* Colloids Surf. A 558, 313–321.

ZHU, X., ZHANG, Y., ZHANG, Y., YAN, Z., NIE, C., LYU, X., TAO, Y., QIU, J., LI, L., 2020. *Flotation dynamics of metal and non-metal components in waste printed circuit boards.* J. Hazard. Mater. 392, 122322.

ZHUO, Q., LIU, W., ZHANG, H., 2020. *Effect of particle size on the relative motion between particles and bubbles*. Colloids Surf. A 601, 124956.